THE UNIVERSITY of EDINBURGH

Edinburgh Research Explorer

Strength characterisation of soil-based construction materials

Citation for published version:
Beckett, CTS, Augarde, CE, Easton, D & Easton, T 2018, 'Strength characterisation of soil-based construction materials', *Géotechnique*, vol. 68, no. 5, pp. 400-409. https://doi.org/10.1680/jgeot.16.P.288

Digital Object Identifier (DOI):
10.1680/jgeot.16.P.288

Link:
Link to publication record in Edinburgh Research Explorer

Document Version:
Peer reviewed version

Published In:
Géotechnique

General rights
Copyright for the publications made accessible via the Edinburgh Research Explorer is retained by the author(s) and / or other copyright owners and it is a condition of accessing these publications that users recognise and abide by the legal requirements associated with these rights.

Take down policy
The University of Edinburgh has made every reasonable effort to ensure that Edinburgh Research Explorer content complies with UK legislation. If you believe that the public display of this file breaches copyright please contact openaccess@ed.ac.uk providing details, and we will remove access to the work immediately and investigate your claim.

Download date: 06. May. 2023

Strength characterisation of soil-based construction materials

C.T.S. Beckett[a,], C.E. Augarde[b], D. Easton[c], T. Easton[c]

[a]School of Civil, Environmental and Mining Engineering, University of Western Australia, Perth, WA 6009
[b]School of Engineering and Computing Sciences, Durham University, Durham, DH1 3LE, UK
[c]Watershed Materials, 11 Basalt Road, Napa, CA 94558, USA

Abstract

Rammed earth (RE) is a venerable construction technique, gaining attention today due to its environmental and sustainable qualities. A key obstacle to its wider adoption is a lack of strength characterisation methods to aid in design and conservation. Research over the past decade has demonstrated that suction is the key mechanism behind strength and strength gain. As suction changes with the building's environment, being able to predict strength changes with suction is essential for practitioners and conservators alike. This paper presents a method for predicting RE strengths based on the Extended Mohr Coulomb (EMC) framework. Construction of an EMC failure envelope in the residual suction range is discussed and the use of a planar envelope justified. Unconfined compression and indirect tensile tests on two RE soils are used to construct this envelope and methods to predict strengths from it are derived. Excellent agreement between measured and predicted strengths is also found for available literature data. Simplifications are identified to adapt the developed technique to suit RE practice and a suitable experimental procedure is outlined. Finally, the revised experimental procedure is employed at an existing RE construction facility to successfully predict strengths of a compacted Californian sandy loam.

Keywords: Rammed earth, suction, Extended Mohr-Coulomb, climate change

1. Introduction

Although the ancient practice of rammed earth (RE) has been demonstrably successful for millennia, the global renaissance of this venerable technique, which is currently underway across the globe, has been hampered by the imposition of engineering standards that are more appropriate to reinforced concrete. In order to secure building code compliance, RE practitioners find themselves required to attain compressive strengths for their installed wall systems (e.g. NZS 4297, Walker and Standards Australia (2002)) that are usually beyond those achievable for soil-based masonry unless Portland cement or other CO_2 generating stabilizers are used to augment the clay-based aggregates.

Clearly, history demonstrates durability for RE that contradicts the strength requirements currently mandated. The RE industry, albeit a small fraction of the more conventional cement-based masonry industry, can benefit from a set of testing protocols that will establish a new set of limits (or standards) from which the testing and permitting agencies can align with the practitioners. Given that unstabilised RE is far more susceptible to strength loss at saturation than stabilized rammed earth, a thorough understanding of the mechanisms that govern strength gain and strength loss in clay-based aggregates is critical to the ultimate success of the industry. Concurrently, RE and other earthen buildings represent a significant proportion of our built heritage. Maintaining this heritage demands a scientific approach to predict and forecast material properties. Therefore, this

Email addresses: christopher.beckett@uwa.edu.au (C.T.S. Beckett), charles.augarde@dur.ac.uk (C.E. Augarde), david@watershedmaterials.com (D. Easton), taj@watershedmaterials.com (T. Easton)

paper sets out to: i) experimentally examine RE strength variation through a comprehensive experimental campaign; ii) develop a framework to predict RE strength change given known environmental conditions; iii) adapt that framework to devise a series of characterisation tests sufficiently simple to be useful for practice.

2. Experimental programme

Suction is a key factor responsible for developing RE's strength and the source of its ability to maintain, in effect, vertical 'slopes' for thousands of years. Understanding the effects of suction variation is therefore critical to any attempt to characterise RE behaviour (Jaquin et al., 2009; Gerard et al., 2015). This section describes the experimental programme developed to investigate RE strength under controlled suction conditions.

2.1. Materials

Site soils can be highly variable and so are inconvenient for laboratory investigations. Instead, 'engineered' soils, manufactured from known quantities of raw materials, were used in this study to guarantee mineralogical and grading consistency. Soils used in this investigation were selected to represent the range of materials used for RE construction around the world are listed in Table 1. Soils were named after their targeted constituent proportions; for example, Soil 4-5-1 nominally comprised 40% silty clay ("Birtley" clay, LL 58.8%, PL 25.7%, 50% kaolinitic clay), 50% sand and 10% gravel by mass. Soils 4-5-1 and 2-7-1 comprised the maximum and minimum recommended silty clay ($\leq 60\mu$m) contents for RE materials respectively (Houben and Guillaud, 1996), to investigate behaviour at the extreme material boundaries. Both soils had the minimum recommended

Table 1: Soil mix constituents, OWC and $\rho_{d,max}$

Soil	Clay (%)	Silt (%)	Sand (%)	Gravel (%)	OWC (%)	$\rho_{d,max}$ (kg/m^3)
4-5-1	19.9	17.2	52.7	10.2	12.0	1940
2-7-1	9.9	9.5	70.7	9.9	12.0	1960

gravel contents (10%) to reduce the influence of large particles on test results and are considered sandy loams by the USDA classification system. Grading curves are given in Figure 1. Soil optimum water contents (OWCs) and maximum dry densities ($\rho_{d,max}$) were determined using the Standard Proctor Test (BS 1377), also given in Table 1.

(Insert Figure 1 somewhere near here)

2.2. Strength testing

The Vapour Equilibrium (VE) method was used to control suction during testing by equilibrating specimens to set temperatures (T) and relative humidities (RH). Under equilibrium conditions, total suction, ψ_t, is controlled by T and RH according to the Kelvin Equation:

$$\psi_t = -\frac{R_u T}{v_m} \ln(\mathrm{RH}) \tag{1}$$

where R_u is the universal gas constant (8.314 J/molK) and v_m is the molar volume of pure water (18.016×10^{-6} m^3/mol). Suction is highly sensitive to seemingly minor changes in atmospheric conditions; by Eqn 1, reducing RH from 70% to 50% at 20°C increases suction from 48.3 to 93.8 MPa.

Strengths at different suction values were examined using a combination of unconfined compression (UCS) and indirect tensile (ITS) testing. UCS is commonly used to compare the performance of different RE soils and so is a technique

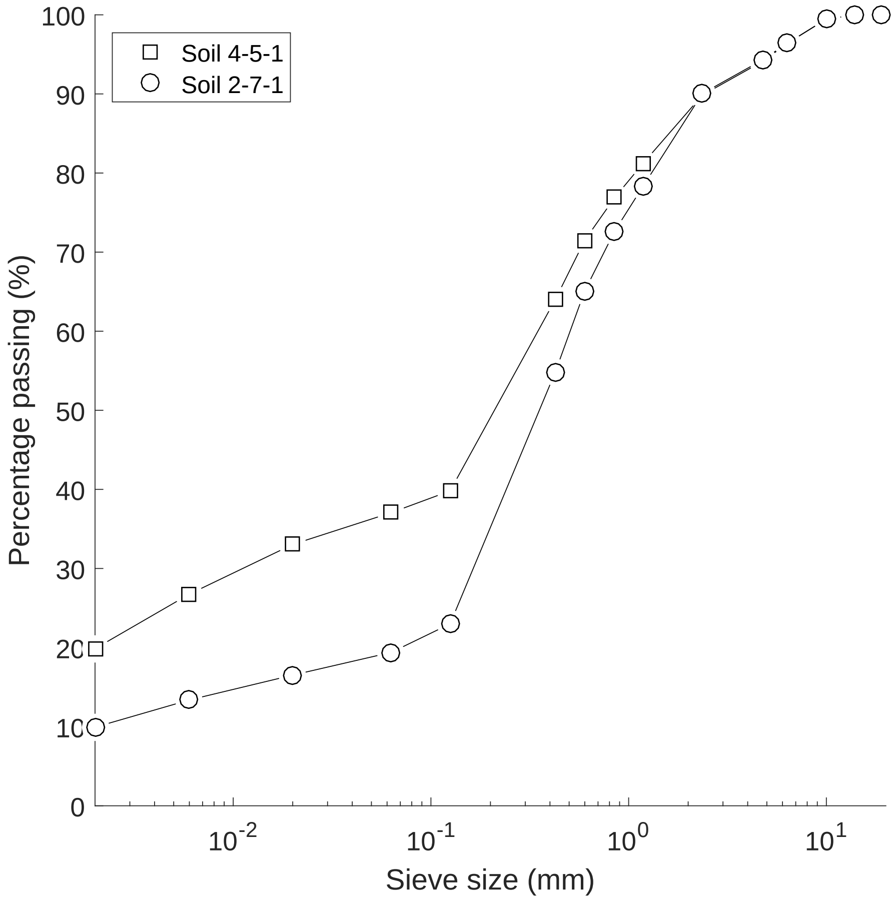

Figure 1: Particle grading curves for mixes 4-5-1 and 2-7-1

already familiar to RE practitioners. ITS was selected as specimen manufacture, handling and testing procedures are similar to those used for UCS testing and so can be accommodated by practitioners' existing facilities and expertise. ITS testing was previously reported in Beckett et al. (2015) but is briefly discussed here for convenience.

2.2.1. UCS testing

100mm cube specimens were manufactured for UCS testing. Although it is common to use $\varnothing 100\times 200$mm cylindrical specimens, the smaller cube specimens were selected to reduce the amount of material needed. UCS specimens were manufactured at the OWC (using deionised water) and to $\rho_{d,max}$ for that mix (Table 1) by compacting three equal layers of known mass to a controlled volume. The upper surface of the specimen was scraped and depressions filled with a screed of fine material (parent soil sieved to pass 0.450mm) to ensure a level surface; this was necessary as specimens could not be rotated to present level surfaces, as is done when testing concrete. Specimens were removed from the mould immediately following manufacture and left to dry on wire racks under conditions of 20 ± 2°C and 45 ± 15% RH until reaching a constant mass for two consecutive days. Specimens were then equilibrated to RH=30, 50, 70 or 90% (± 3%) and T =15, 20, 30 or 40°C (± 2°C) (14–174MPa suction by Eqn 1) using an environmental chamber (EC, Vötsch VC4033). An initial drying period was necessary prior to equilibration due to limited EC availability and difficulties in transporting fresh specimens. Specimens therefore either gained or lost water to achieve their final equilibration: consequences of testing specimens under wetting or drying conditions are discussed in the following sections. Once equilibrated, specimens were immediately transferred to a testing machine and uniaxially loaded at a controlled displacement rate of 0.5mm/min until failure. Specimens were not capped as surfaces were level. Specimen water contents were determined by oven drying crushed material. Three specimens were manufactured per RH and T combination per soil; 96 in total.

RH and T values were selected to be representative of typical atmospheric conditions at RE sites around the world (Beckett and Augarde, 2012). However, moisture contents can also be affected by incident rainfall or capillary rise (Hall and Djerbib, 2004). Under such circumstances, suction values are likely to fall below those examined here. However, these events constitute failures of the structural design, so that material would not be exposed to such conditions under normal circumstances. Consequences of suctions falling significantly below examined levels are discussed in the following sections. It should also be noted that UCS specimens behaved as soil elements due to equilibration to constant suction conditions. In practice, water content gradients may exist through RE structural components due to hygrothermal interactions with the surrounding atmosphere (McGregor et al., 2015). As such, our testing programme was not representative of *structural* element behaviour but can be used to assess potential strength changes along a moisture or suction gradient.

2.2.2. ITS testing

$\varnothing$100×50mm ‘disc’ specimens were manufactured following a similar procedure to that for UCS specimens. Specimens were removed from the mould and air-dried on wire racks to a target water content, then wrapped in clear plastic for a minimum of two days for suction equilibration. Specimens were tested to failure at a displacement rate of 0.2mm/min between curved metal platens. Manufacturing and orientating specimens in this way tested indirect tensile strength perpendicular to the compaction planes (Beckett et al., 2015). Tensile strength, σ_t, was determined via

$$\sigma_t = -\frac{P}{\pi R L} \tag{2}$$

where P is the applied compressive load and R and L are the specimen radius and length respectively. Eqn 2 is valid for specimens with little deformation (Frydman, 1964). The highest suctions achieved from air-drying ITS specimens were 60 and 80 MPa for Soils 4-5-1 and 2-7-1 respectively. The minimum suction was roughly 1 MPa for both soils. Again, ITS testing was representative of soil, rather than structural, elements.

2.3. Soil water retention properties

Soil-water retention properties for Soils 4-5-1 and 2-7-1 were reported in Beckett et al. (2015). For convenience, the procedures used are briefly discussed here. Drying retention properties were determined using a combination of filter paper (suctions 0 to 4 MPa) and vapour-equilibrium (10 to 200 MPa) methods. Filter paper testing followed ASTM D5298-10. The relationship

$$\ln \psi_t = -4.6234 - 3.6454 \ln(w_{fp}) \tag{3}$$

was used to calculate ψ_t from the gravimetric water contents (w_{fp}) of suspended filter papers (i.e. those in equilibrium with the surrounding air), determined via a best-fit relationship to data presented in Hamblin (1981). Soil water retention curves (SWRCs) for each mix are shown in Figure 2, where data were fitted using

$$C = \left(1 + \frac{\log\left(1 + \frac{\psi_t}{10^9}\right)}{\log(2)}\right) \quad (4)$$

$$S_r = C \times \frac{1}{\left(\ln\left(\epsilon + \left(\frac{\psi_t}{a}\right)^n\right)\right)^m} \quad (5)$$

where S_r is the degree of saturation, ϵ is the Euler number, C is a correction term limiting S_r to 0 at $\psi_t = 1$GPa and a, m and n are fitting parameters given in Figure 2 (Fredlund and Xing, 1994). Residual suction values (ψ_{res}) were found from intersecting lines drawn tangentially to the steepest and shallowest parts of the curve. Although it is common to impose that the latter tangent passes through $S_r = 0$ at $\psi_t = 1$GPa, the correction term in Eqn 5 causes bimodality in the high suction portion of the SWRC, producing an unrealistic estimation of ψ_{res}; tangents to the shallowest section of the curve were therefore used. ψ_{res} and $S_{r,res}$ are given in Figure 2.

(Insert Figure 2 somewhere near here)

3. Experimental results

UCS values for Soils 4-5-1 and 2-7-1 are shown in Figures 3 and 4 respectively. Note that UCS was not factored to account for the use of cubic, rather than the more common cylindrical, specimens. ITS results for untreated Soils 4-5-1 and 2-7-1 from Beckett et al. (2015) are shown in Figure 5.

Figures 3 to 5 show that UCS roughly doubled and ITS increased tenfold between the lowest and highest tested suction conditions for both soils. It is possible that an RE structure might experience the full range of these conditions over the course of a single year; given their large surface area, equilibration to such

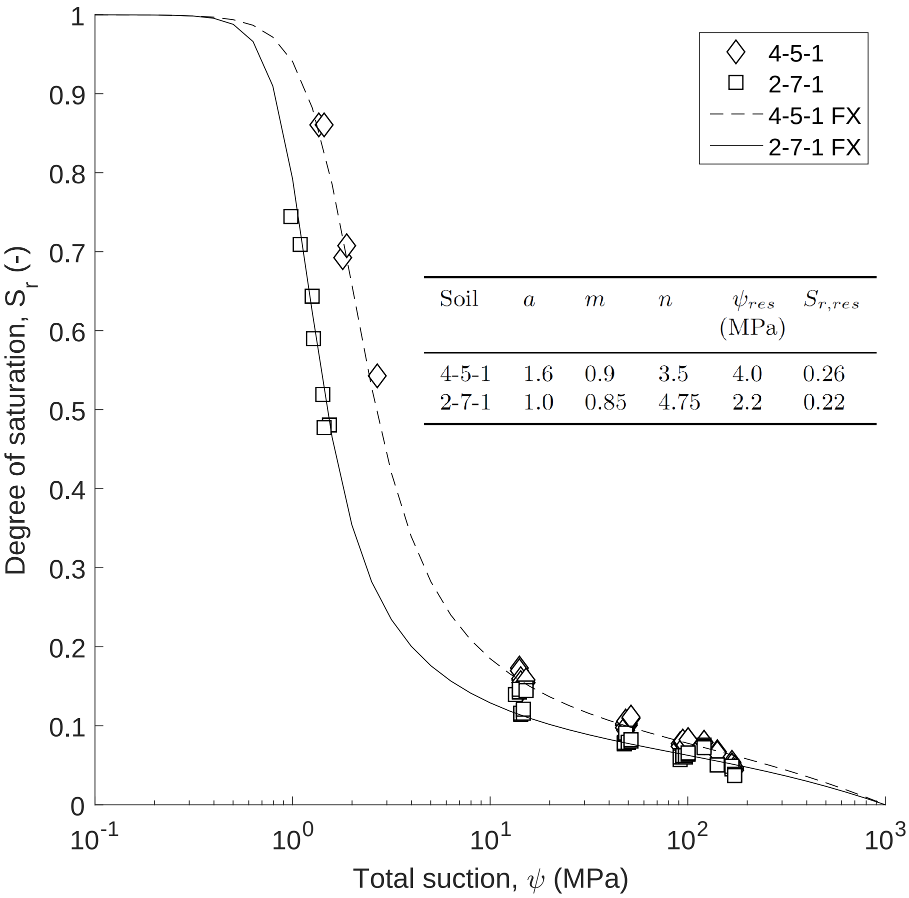

Soil	a	m	n	ψ_{res} (MPa)	$S_{r,res}$
4-5-1	1.6	0.9	3.5	4.0	0.26
2-7-1	1.0	0.85	4.75	2.2	0.22

Figure 2: Soil 4-5-1 and 2-7-1 drying retention curves and fitting parameters. FX: fit using Eqn 5

conditions is rapid and large changes in strength over a building's life may result. Suction variation must therefore form the basis of any strength characterisation methods. The development of such a method is discussed in the following sections.

(Insert Figure 3 somewhere near here)

(Insert Figure 4 somewhere near here)

(Insert Figure 5 somewhere near here)

4. Constitutive model development

4.1. Extended Mohr-Coulomb failure criterion in the residual suction range

Two common approaches exist to incorporate suction into an effective stress framework. The generalised effective stress method uses an effective stress parameter, χ, to modify the existing pore water pressure term:

$$\sigma' = \sigma - \chi(u_a - u_w) \tag{6}$$

where u_a and u_w are the pore air and water pressures respectively. The advantage of Eqn 6 is that it is similar in construction to the Terzaghi effective stress approach familiar to most geotechnical engineers. However, the form of χ is disputed and heavily dependent on the form of the SWRC (Khalili and Khabbaz, 1998). An alternative to this approach is to introduce suction as a third stress state variable (Fredlund and Morgenstern, 1977). Shear strength is calculated via

$$\tau_f = c' + (\sigma - u_a)\tan\phi + (u_a - u_w)\tan\phi^b \tag{7}$$

where c' is the effective cohesion, ϕ' is the effective friction angle and $\tan\phi^b$ describes the change in shear strength with suction at a constant value of net

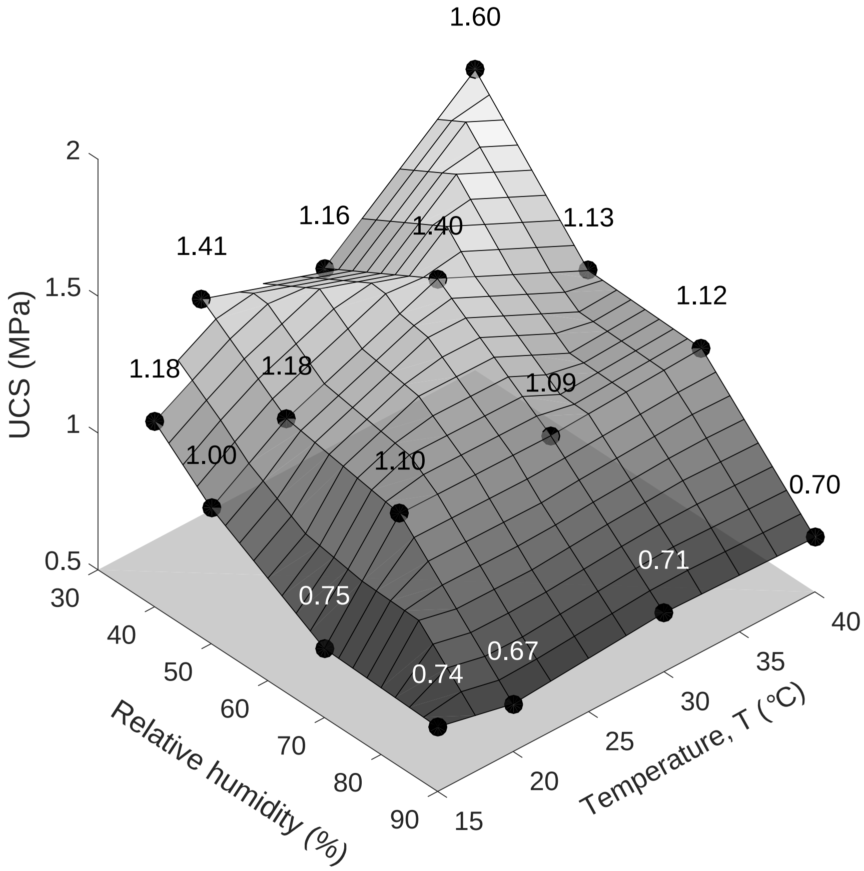

Figure 3: UCS results for Soil 4-5-1 (individual values shown above markers)

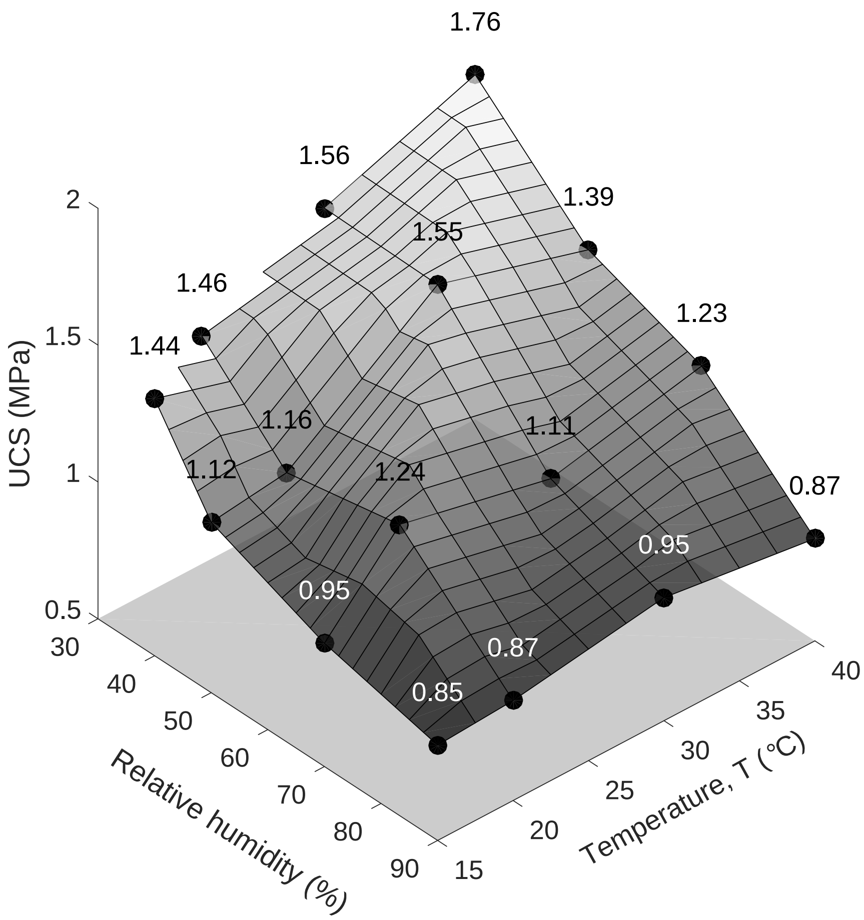

Figure 4: UCS results for Soil 2-7-1 (individual values shown above markers)

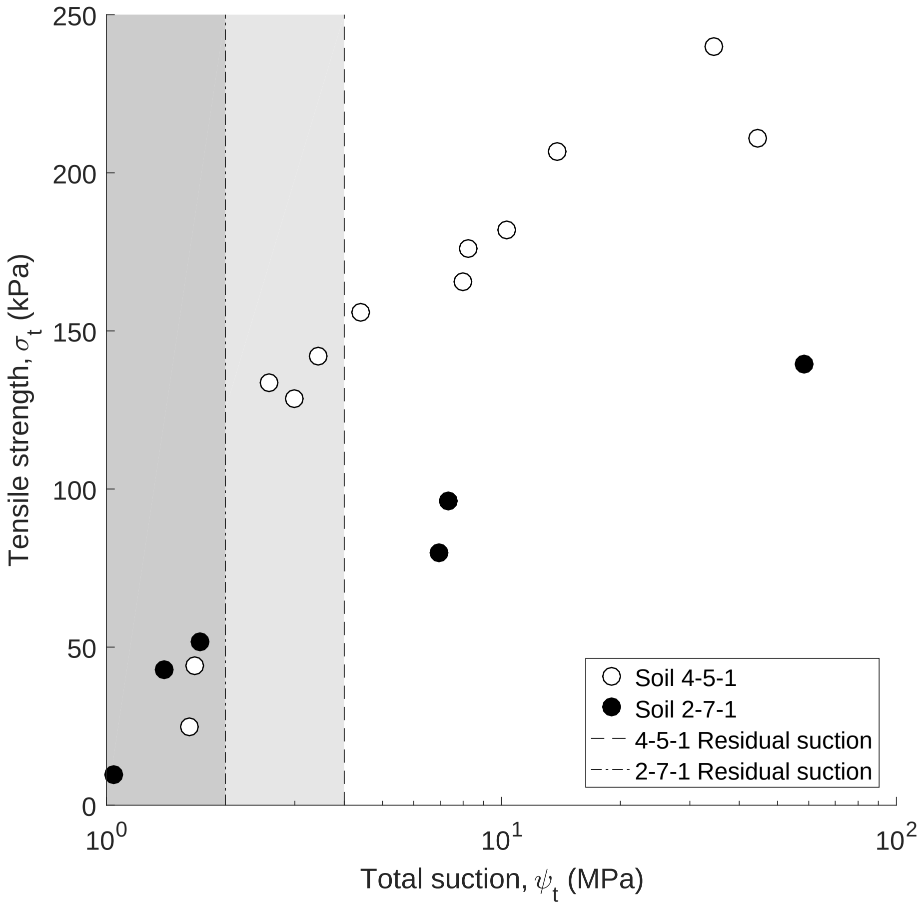

Figure 5: ITS results for Soils 4-5-1 and 2-7-1 from Beckett et al. (2015). Shaded regions show suctions below residual values

stress $(\sigma - u_a)$. It is generally accepted that ϕ^b is a function of S_r and diminishes to small values as S_r approaches zero (Gan et al., 1988; Fredlund and Rahardjo, 1993). The advantage of this "extended" Mohr-Coulomb criterion (EMC) is that the contributions of suction and net stress can be assessed separately.

ϕ' is commonly assumed to be constant in the residual suction range (Fredlund et al., 1987). However, the form of ϕ^b depends on the range of suction investigated. Fredlund et al. (1996) and Vanapalli et al. (1996) presented a method to predict values of ϕ^b from ϕ' for given values of suction, via

$$\tan\phi^b = \left(\Theta(\psi)^\kappa + \psi \frac{d\left(\Theta(\psi)^\kappa\right)}{d\psi}\right)\tan\phi' \tag{8}$$

where $\Theta = \dfrac{\theta(\psi) - \theta_{res}}{\theta_s - \theta_{res}}$, $\theta(\psi)$, θ_s and θ_{res} are the volumetric water contents at the current, saturation and residual suction values respectively and κ is a fitting parameter. As $\Theta \leq 1 \; \forall \; \psi$, Eqn 8 maintains $\phi^b < \phi'$ for suctions above the air-entry value as discussed above. To avoid negative values of Θ for $\theta < \theta_{res}$, Eqn 8 can be simplified by assuming $\theta_{res} = 0$ so that $\Theta = S_r$, i.e.

$$\tan\phi^b = \left(S_r(\psi)^\kappa + \psi \frac{d\left(S_r(\psi)^\kappa\right)}{d\psi}\right)\tan\phi'. \tag{9}$$

Depending on the expression used for the SWRC (e.g. Eqn 5), $\frac{d(S_r^\kappa)}{d\psi}$ in Eqn 9 can be quite complex. However, assuming a linear SWRC in the residual suction range (as supported by Figure 2) reduces $\frac{d(S_r(\psi)^\kappa)}{d\psi}$ to a constant value. As $\frac{d(S_r(\psi)^\kappa)}{d\psi}$ is small, $S_r(\psi)^\kappa$ is also nominally constant. Therefore, in the residual suction range, we assumed ϕ^b to be constant and so the failure envelope to be planar.

Table 2: EMC parameters determined for RE soils

Soil	c' (MPa)	ϕ' (°)	ϕ^b (°)	ϕ^b (°, Eqn 9)	κ (Eqn 9)	Fitted suction range (MPa)
4-5-1	0.24	24.5	0.082	0.084	1.25	4.0–60
2-7-1	0.15	39.7	0.093	0.092	1.44	4.0–80

4.2. Modelling experimental data

UCS data discussed above and ITS results for untreated material from Beckett et al. (2015) were used to construct EMC failure surfaces for Soils 4-5-1 and 2-7-1. Construction of the failure envelope from UCS and ITS data is shown schematically in Figure 6. The final fitted plane for 2-7-1 is shown in Figure 7. Mohr's circles for UCS tests were drawn assuming that $\sigma_2 = \sigma_3 = 0$ and $\sigma_1 = \sigma_c$. ITS Mohr's circles were drawn assuming $\sigma_2 = 0$, $\sigma_3 = \sigma_t$ and $\sigma_1 = -3\sigma_t$ (noting that σ_t is negative in Eqn 2). ITS relationships were derived in Li and Wong (2013) and are valid for specimens with little deformation, as is the case for such high suction values. Circles were discretised and points for best plane fitting were determined via a least squares approach. Planes were fitted using the suction range for which both UCS and ITS data were available. c', ϕ' and ϕ^b and the fitted suction range for each soil are given in Table 2.

(Insert Figure 6 somewhere near here)

ϕ' values in Table 2 were similar to those typically found for compacted sandy loam soils, e.g. Vanapalli et al. (1996). Although ϕ^b values were close to zero, as expected for results in the residual suction range, the contribution of ϕ^b to strength was significant due to the high values of suction present. κ was selected to produce the best match between experimental ϕ^b values and those found via Eqn 9 using experimentally-derived ϕ' and SWRCs. κ fell within the κ =1–3 limits suggested by Fredlund et al. (1996) for both soils, supporting the assumption

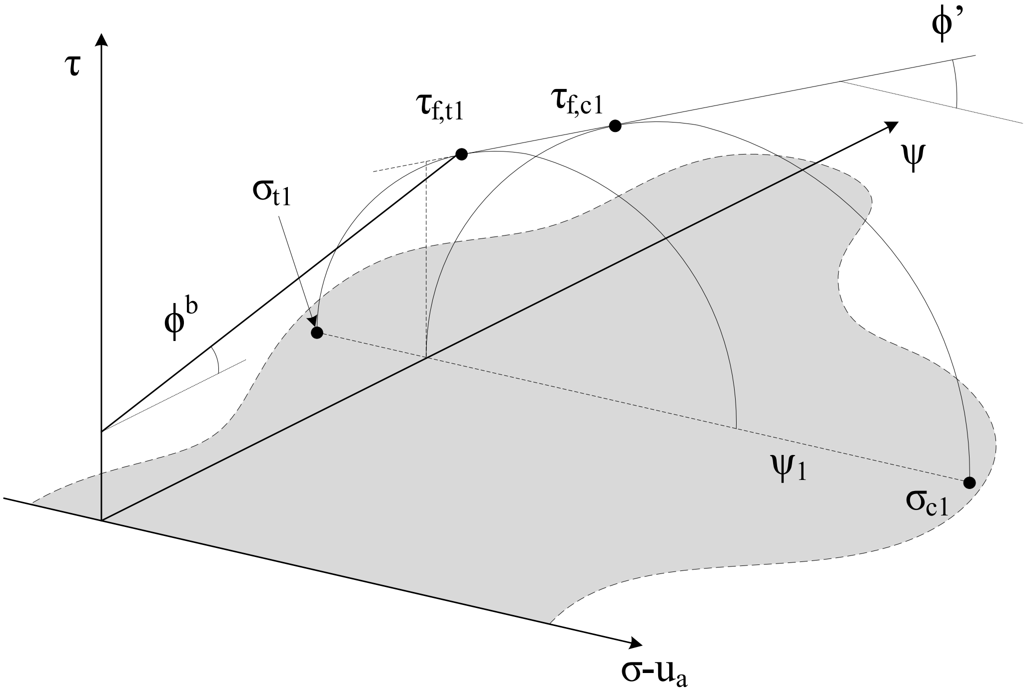

Figure 6: Construction of the planar EMC failure envelope using UCS and ITS data

of a planar failure envelope in the residual suction range. Although Soil 2-7-1 achieved a higher UCS for all tested suction values, the fitted plane had a lower c' value than for Soil 4-5-1; this was due to the poor performance of Soil 2-7-1 in tension. Soil 2-7-1's lower c' was countered by higher ϕ' and ϕ^b values. A higher ϕ' value was likely due to Soil 2-7-1's higher dry density and so greater particle interlock. The higher ϕ^b value was due to a shallower retention curve in the residual range, diminishing the contribution of the term in parentheses (negative) in Eqn 9.

(Insert Figure 7 somewhere near here)

UCS can be predicted from fitted c', ϕ' and ϕ^b values via

$$\text{UCS} = 2\left(\frac{c' + \psi \tan\phi^b}{\cos\phi' - (1 - \sin\phi')\tan\phi'}\right) \tag{10}$$

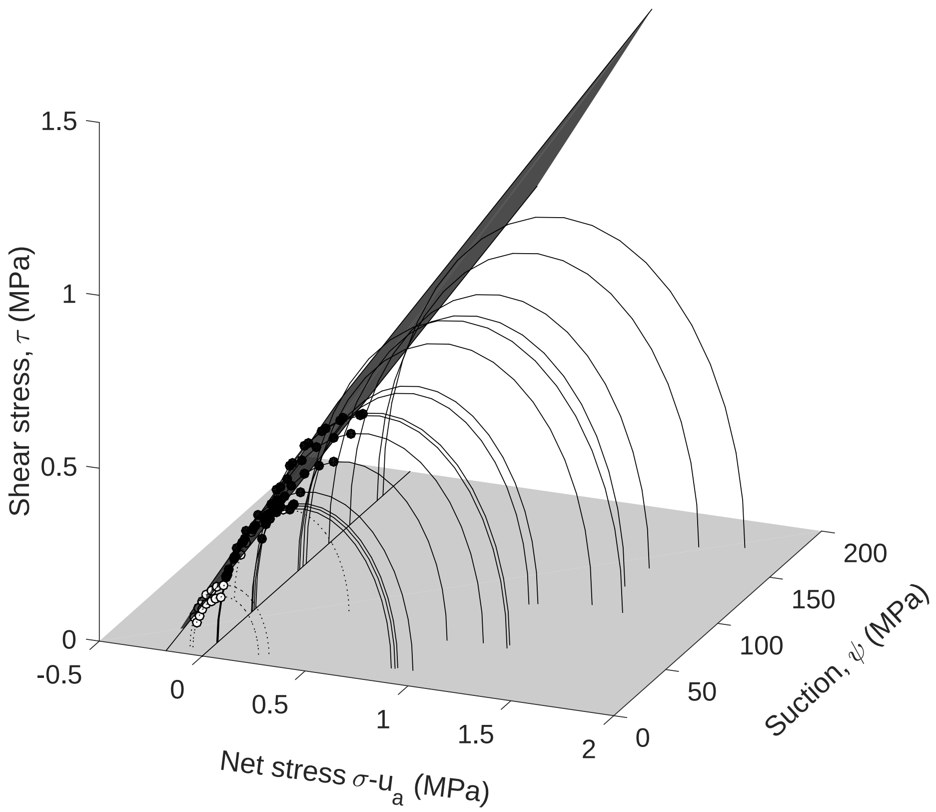

Figure 7: Soil 2-7-1 planar EMC failure envelope. - UCS results; - - ITS results. Markers denote points on the circles used for plane fitting. Mohr's circles without markers fell outside the ITS suction range

Eqn 10 is similar to that proposed by Panayiotopoulos (1996) to find UCS using the generalised effective stress approach, however it maintains a clear distinction between the suction (the numerator) and internal friction (the denominator) contributions to UCS. Figure 8 compares measured UCS values for mixes 4-5-1 and 2-7-1 and those predicted via Eqn 10. Predictions fall evenly about the line of equality ($\pm$0.15 MPa). Notably, there was no significant change in prediction accuracy for UCS values above the upper ITS suction limit (i.e. above the range for which plane fitting was defined) for either soil. Good accuracy beyond the fitted range was due to the near-linear SWRC for suctions above the residual value. Given the sensitivity of the SWRC gradient to the correction term in Eqn 5 in the residual range, it is likely that the quality of fit would reduce for suctions much higher than those tested. The fit quality would also suffer for suctions below the residual value, for example as might arise during capillary rise. However, for the range investigated, a planar failure envelope was suitable.

(Insert Figure 8 somewhere near here)

4.3. Application to literature data

Few suction-dependent RE strength datasets are available in the literature. However, RE water retention and UCS data were presented in Jaquin et al. (2009), Bui et al. (2014) and Gerard et al. (2015). Properties of those soils are given in Table 9. Failure planes were fitted to Mohr's circles constructed from UCS and suction data in the residual suction range, as judged by SWRCs in those works, using the procedures discussed in the previous section. As only UCS data was available for data in Jaquin et al. (2009) and Bui et al. (2014), plane fitting was forcibly restricted to $\phi', \phi^b > 0$. The full procedure was implemented for data from Gerard et al. (2015). c', ϕ' and ϕ^b values for these soils are given in Table 4

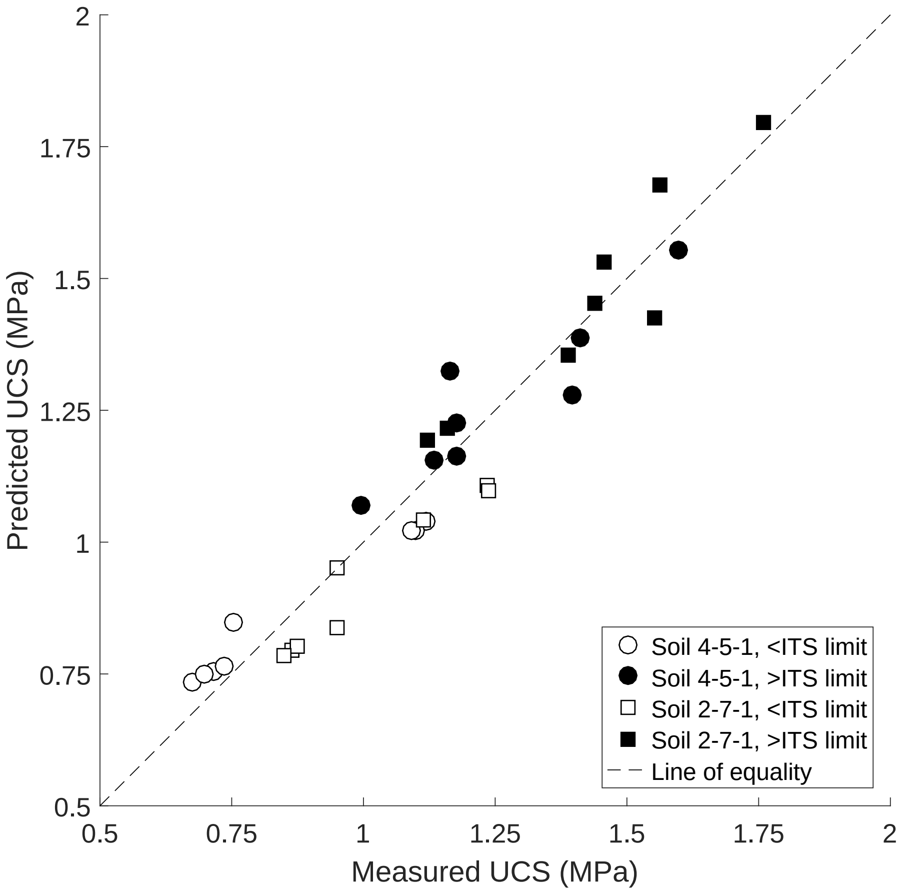

Figure 8: Comparison of measured and predicted UCS above and below ITS suction limit

Table 3: Constituents of soils used in the literature. CWC: Compaction Water Content. *Stabilised with 2% natural hydraulic lime. **Predominantly kaolinitic. ***Predominantly montmorillonitic

Soil	Clay (%)	Silt (%)	Sand (%)	Gravel (%)	CWC (%)	$\rho_{d,max}$ (kg/m^3)
Jaquin et al. (2009)	—15**—		25	60	12	2040
Bui et al. (2014) Soil A	5***	30	49	16	11	1920
Bui et al. (2014) Soil B*	4***	35	59	2	11	1920
Bui et al. (2014) Soil C	9***	38	50	3	11	1920
Gerard et al. (2015)	13**	64	26	0	15	1840

and measured and predicted UCS values are compared in Figure 9. ϕ^b values were larger than those in Table 2 due to the narrower fitted suction range. Excepting Bui et al. (2014) Soil C, κ values outside of the 1–3 limit were required to match experimental and predicted ϕ^b values, most notably for Jaquin et al. (2009). By Eqn 9, a low κ value indicated little contribution of suction or saturation changes to changes in ϕ^b, so that $\phi^b \approx \phi'$ as is expected at low suction. That values marginally outside the 1–3 limit were needed to fit other soils is reasonable given the restriction to UCS results only for Bui et al. (2014) or the extremely high strengths found in Gerard et al. (2015). Notably, the fit quality was seemingly unaffected the presence of stabiliser (Bui et al. (2014) Soil B); this was perhaps to be expected, given the low stabiliser and clay contents (for lime, the latter is required for the former to react) and the strong contribution of suction to strength for weakly lime-stabilised RE (Ciancio et al., 2014).

(Insert Figure 9 somewhere near here)

5. Adaptation to practice

At present, RE construction is hampered by a lack of construction codes or standards and a shallow pool of available contractors. It is therefore unrealistic to assume that RE practitioners can perform a wide range tests for every potential

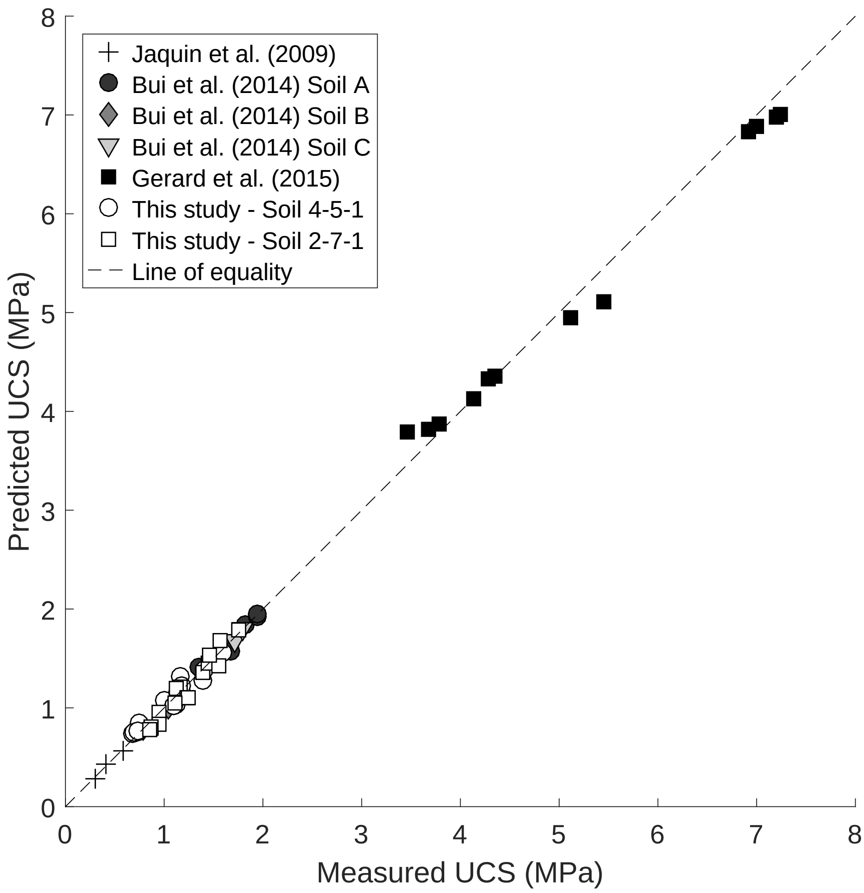

Figure 9: Measured and predicted UCS values for literature soil data

Table 4: EMC parameters derived for literature soils

Soil	c' (kPa)	ϕ' ($^\circ$)	ϕ^b ($^\circ$)	ϕ^b ($^\circ$, Eqn 9)	κ (Eqn 9)	Suction range (MPa)
Jaquin et al. (2009)	83.1	11.42	10.62	10.62	0.09	0.18–0.80
Bui et al. (2014) Soil A	512.7	11.92	0.24	0.24	3.72	3.2–65
Bui et al. (2014) Soil B	267.7	11.34	1.03	1.04	0.93	3.2–11
Bui et al. (2014) Soil C	566.2	12.63	0.25	0.25	1.25	8.1–36
Gerard et al. (2015)	929.4	38.5	0.32	0.32	3.07	4.1–126

RE soil or can afford the cost and delay of a lengthy laboratory campaign. To be useful to RE industry, the EMC method discussed above can be simplified in three key areas: i) tangential plane selection; ii) plane fitting; iii) testing equipment.

5.1. Plane selection

A complex (and potentially subjective) step of the plane-fitting process is identifying the most accurate tangent to the Mohr's circles. An alternative to a tangential failure envelope is to draw the envelope passing through the circle maxima, as shown in Figure 10 where subscripts c and t denote compression and tension respectively (Fredlund and Rahardjo, 1993). The advantage of this approach is that only one point per circle need be identified for plane fitting. UCS can be predicted from fitted c', ϕ^* and ϕ^B values via

$$\mathrm{UCS} = 2\left(\frac{c' + \psi \tan\phi^B}{1 - \tan\phi^*}\right) \tag{11}$$

as derived in the Appendix. Note that $\phi^* \equiv \phi'$ and $\phi^B \equiv \phi^b$ in function for the failure envelope defined using circle maxima. $\phi^* \neq \phi'$ and $\phi^b \neq \phi^B$, however they are similar for most soils (Powrie, 2008).

(Insert Figure 10 somewhere near here)

To examine the validity of the simplified approach, UCS values for Soils 4-5-1 and 2-7-1 were re-predicted using Eqn 11. Measured and predicted values are compared in Figure 11. As for Figure 8, distinctions were made between strengths at suctions above and below the maximum ITS suction. With the exception of one result for Soil 4-5-1, results fall largely between the line of equality and an overprediction of roughly 0.15 MPa. The simplified method is therefore no less accurate, within the confines of available results, than the

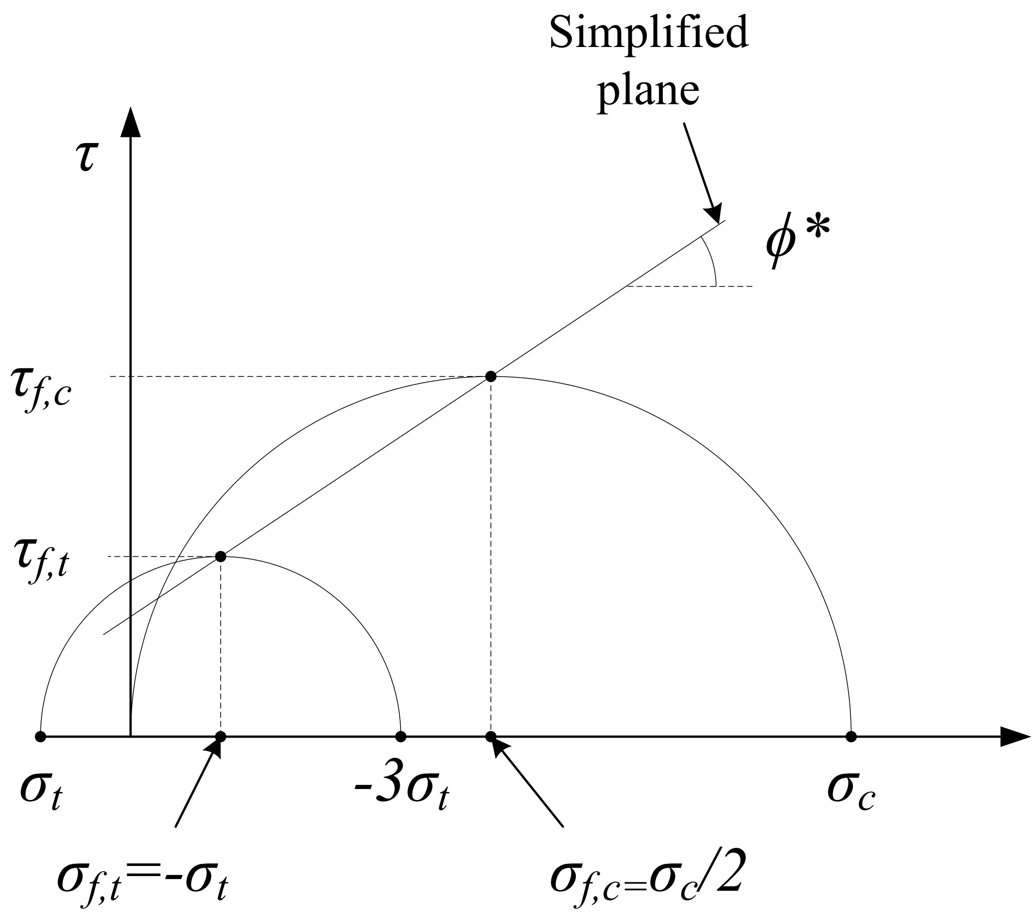

Figure 10: Construction of EMC failure envelope using circle maxima

full method. Strength overprediction is not conservative, however the amount is minor and can be accommodated by any reasonable margin of safety.

(Insert Figure 11 somewhere near here)

5.2. Plane fitting

Plane-fitting requires powerful computer software, for example MATLAB. That practitioners and laboratories will have access to such software or expertise in its use is unlikely. The fitting process can be significantly simplified by only testing specimens at the plane 'corners', i.e. performing UCS and ITS tests at the minimum and maximum anticipated suction conditions. That this is valid was demonstrated by the good agreement for predictions above the ITS suction limit in Figure 8. ϕ^*, ϕ^B and c' calculations using this simplified method are derived in the Appendix. UCS can then be calculated using Eqn 11 as before.

5.3. Testing equipment and revised experimental procedure

Environmental chambers are large, expensive pieces of equipment and therefore uncommon in most laboratories. An inexpensive alternative is to use saturated salt solutions to equilibrate specimens to target suction values. Potential solutions and corresponding suction values are given in Table 5 (Hall and Allinson, 2009). Using this technique, a sealable container is partially filled with the salt solution and the specimen suspended above it until it reaches constant mass. Furthermore, the ITS 'discs' used here are not commonly encountered in practice. Cylinders of the same dimensions used for UCS testing can be substituted for the discs; σ_t is given by Eqn 2 as before.

Based on these simplifications, an experimental procedure readily accessible and relevant to practitioners can be outlined:

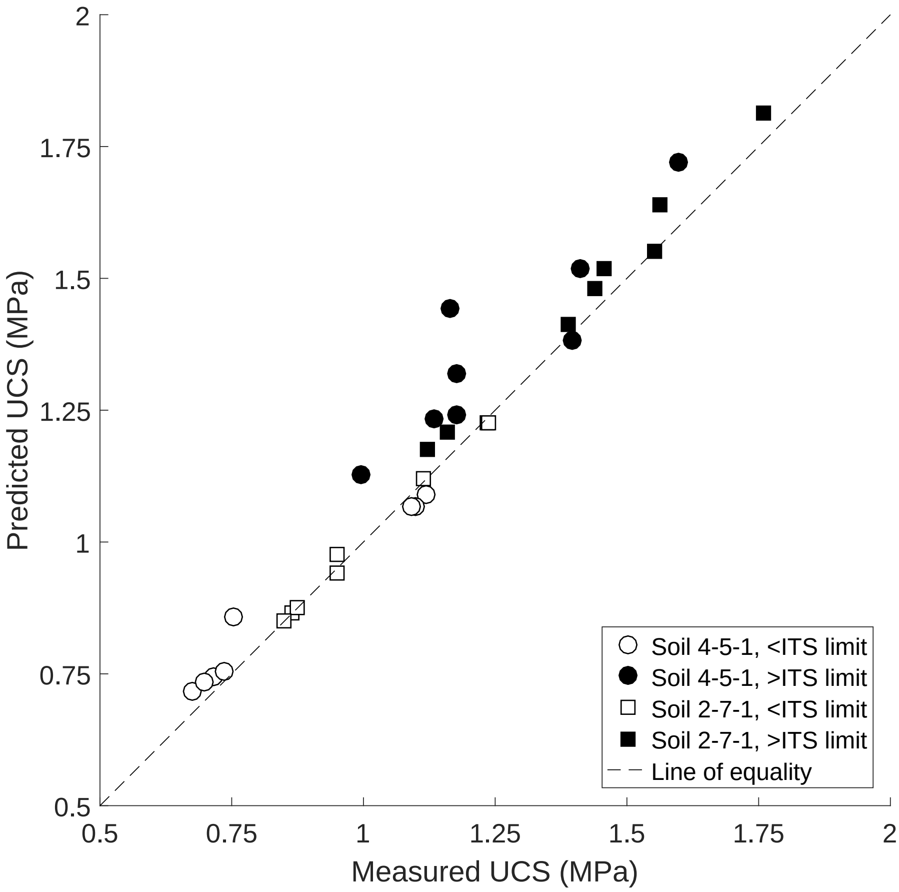

Figure 11: Comparison of measured and predicted UCS values found using the simplified EMC method

Table 5: Saturated salt solutions, associated RH and equivalent suction values for specimen suction equilibration (Hall and Allinson, 2009)

Salt solution	RH at 23°C	Suction (MPa)
Magnesium chloride	32.9±0.2	203.2
Potassium chloride	43.2±0.4	153.4
Magnesium nitrate	53.5±0.2	114.3
Sodium bromide	58.2±0.4	98.9
Sodium chloride	75.4±0.1	51.6
Potassium nitrate	94.0±0.6	11.3

1. Determine optimum compaction conditions for the proposed soil using standard testing methods (e.g. AS1289, BS1377 etc.).
2. Obtain ambient site RH and T data (e.g. from government meteorological agencies) and calculate likely minimum and maximum suction conditions using Eqn 1.
3. Identify suitable salt solutions for this suction range (Table 5).
4. Manufacture three specimens (at the optimum compaction conditions) per suction condition for UCS and ITS testing.
5. Seal specimens in containers and periodically check mass until it becomes constant.
6. Test specimens for UCS or ITS using methods described in this paper. UCS or ITS is the average of the three specimen strengths.
7. Calculate c', ϕ^* and ϕ^B using simplified EMC method (Eqns 20 to 28).
8. Use EMC parameters to predict strengths for suction range of interest (Eqn 11).

5.4. Implementation of simplified testing programme

To test its flexibility, the simplified testing programme outlined above was implemented at an RE construction facility (Watershed Materials) in California, USA. ∅150×300mm UCS and ITS specimens were manufactured from a local rock aggregate, modified with 25% "C-Red" clay by mass (LL 24.1%, PL 16.2%, predominantly kaolinitic with a high iron content). Cylindrical specimens were selected for consistency with preferred industry practice. The final material's particle grading curve is shown in Figure 12. OWC (7.8%) and $\rho_{d,max}$ (2100kg/m^3) were determined following ASTM-D1557. Specimens were equilibrated at high and low humidities (93% and 34%) at 20°C, equivalent to 9.81 and 145.9 MPa suction respectively, using the above techniques, and tested in either compression or tension on reaching constant mass. Three specimens were prepared per condition (12 in total).

(Insert Figure 12 somewhere near here)

To test the procedure's ability to successfully predict strength across the suction range, a failure plane was fitted to ITS results and UCS results at low suction only (i.e. using only three of the four 'corners' to define the plane). UCS and ITS results and the best-fitted failure plane to the selected Mohr's circles (using circle maxima) are shown in Figure 13. EMC parameters are given in Table 6; c', ϕ^* and ϕ^B values were similar to equivalent parameter values found for Soils 4-5-1 and 2-7-1, likely due to the similar soil textures, densities and suction range. Agreement between the two indicated that the simplified procedure was able to capture reliable and representative EMC parameters; in the absence of a SWRC, however, ϕ^B predictions using Eqn 9 could not be made. Strengths predicted from the restricted dataset are compared to those found by fitting a plane to all available data in Figure 14. As expected, excellent agreement was found between predicted and measured values using the full dataset due to the fitting nature of the procedure. Using the restricted dataset, predicted strengths were, at most, 0.1MPa higher than measured values, i.e. within the anticipated accuracy found

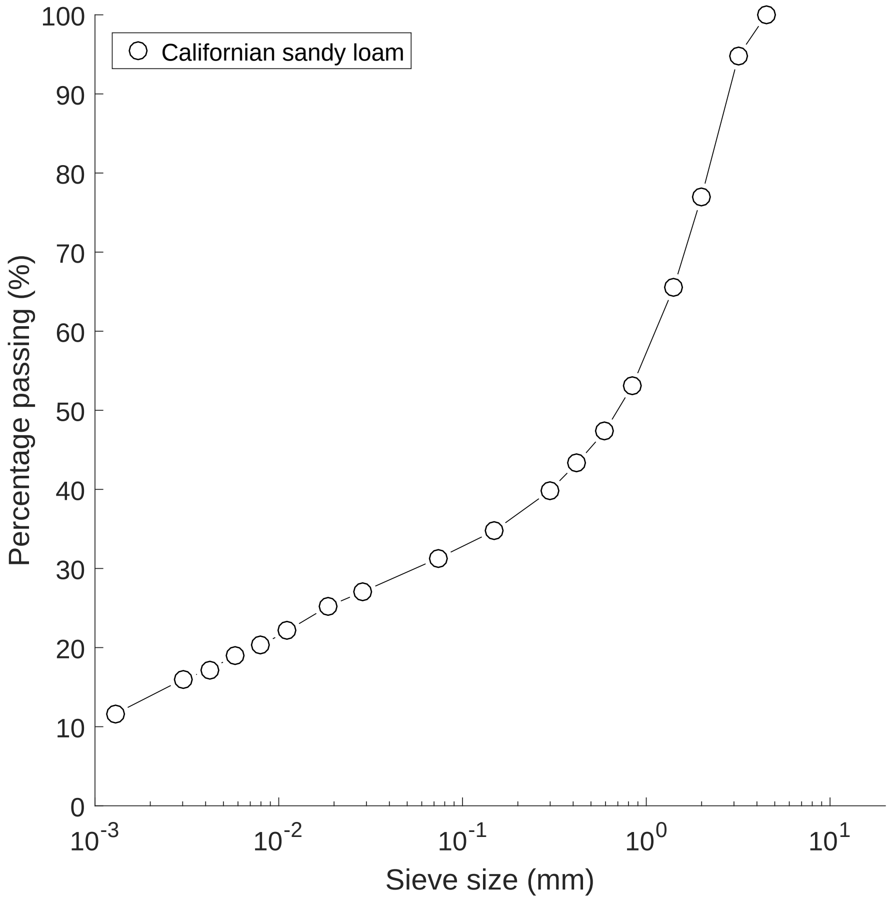

Figure 12: Particle grading curve for modified Californian sandy loam

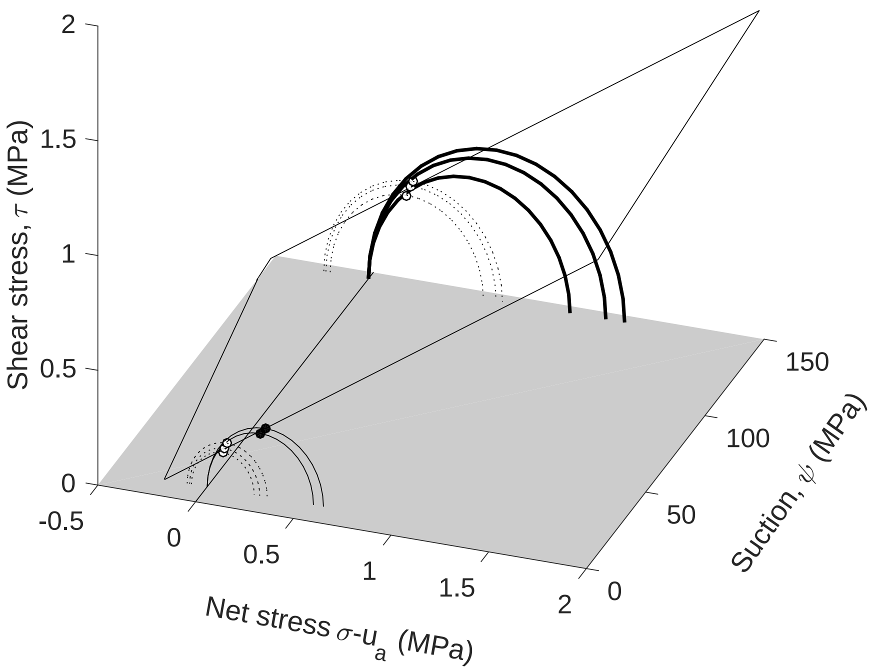

Figure 13: Planar EMC failure envelope for the Californian sandy loam. - UCS results; - - ITS results. Markers denote points on the circles used for plane fitting. Bold circles were omitted from plane-fitting for comparison to predicted values. Note that one UCS specimen at low suction was damaged prior to testing and so was not included

for the full procedure.

(Insert Figure 13 somewhere near here)

(Insert Figure 14 somewhere near here)

6. Conclusions

Strength uncertainty is a critical obstacle preventing RE's use in wider engineering and construction practice. Recent research has demonstrated that suction

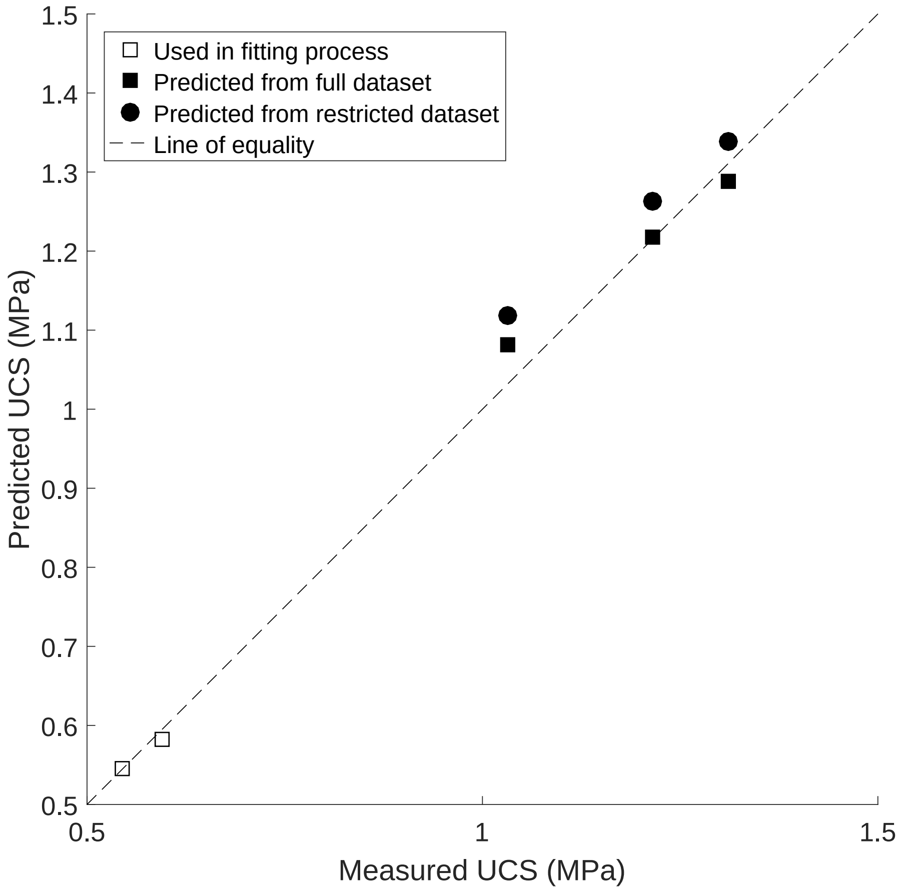

Figure 14: Comparison of measured and predicted UCS values for the Californian sandy loam found using the simplified EMC method and a restricted or complete dataset

Table 6: EMC parameters derived for the Californian sandy loam using the restricted and full dataset

Soil	c' (kPa)	ϕ' (°)	ϕ^b (°)	Suction range (MPa)
Restricted dataset	112.7	30.0	0.075	9.81–145.9
Full dataset	128.6	25.9	0.073	9.81–145.9

is a key element controlling strength development in these materials. Developing a technique to reliably and realistically characterise strengths is key to improving confidence in RE design, construction and conservation programmes.

This paper presents suction-controlled UCS and ITS results for soils representative of the range and mineralogies likely to be used for RE construction. Strengths were found to almost double between the lowest and highest suctions for both soils. The EMC method was introduced to describe and predict strength changes with suction. Construction of the failure envelope was discussed and the use of a planar failure envelope in the residual suction range justified. Using this technique, good agreement ($\pm$0.15 MPa) was found between measured and predicted strengths for both tested soils across the entire suction range. Good agreement was also found when the technique was applied to literature data of varying suction ranges. Simplifications to the failure plane selection, fitting and experimental techniques were identified to adapt the developed technique to suit RE practice. The simplified plane selection and fitting techniques were tested on UCS and ITS data with no demonstrable loss in accuracy. Finally, the simplified experimental procedure was used to investigate strengths of a compacted Californian sandy loam tested at an existing RE construction facility. The simplified technique successfully predicted strengths over the entire suction range with the same accuracy as found for the full method.

Acknowledgements

The first author was supported by a studentship awarded by the School of Engineering and Computing Sciences, Durham University whilst this research was undertaken and is now supported by ARC Linkage Grant LP140100375.

References

ASTM, 2010. ASTM D5298-10. Standard test method for measurement of soil potential (suction) using filter paper.

Beckett, C. T. S., Augarde, C., 2012. The effect of relative humidity and temperature on the unconfined compressive strength of rammed earth. In: Mancuso, C., Jommi, C., D'Onza, F. (Eds.), Unsaturated Soils: Research and Applications. Second European Conference on Unsaturated Soils. Springer Berlin Heidelberg, pp. 287–292.

Beckett, C. T. S., Smith, J. C., Ciancio, D., Augarde, C. E., 2015. Tensile strengths of flocculated compacted unsaturated soils. Géotechnique Letters 5 (4), 254–260.

BSI, 1990. BS 1377:1990. Methods of testing for soils for civil engineering purposes.

Bui, Q.-B., Morel, J.-C., Hans, S., Walker, P., 2014. Effect of moisture content on the mechanical characteristics of rammed earth. Construction and Building Materials 54, 163–169.

Ciancio, D., Beckett, C. T. S., Carraro, J., 2014. Optimum lime content identification for lime-stabilised rammed earth. Construction and Building Materials 53, 59–65.

Fredlund, D., Rahardjo, H., 1993. Soil mechanics for unsaturated soils. John Wiley & Sons Inc., New York (USA).

Fredlund, D. G., Morgenstern, N. R., 1977. Stress state variables for unsaturated soils. Journal of the Geotechnical Engineering Division 107 (GT5), 447–466.

Fredlund, D. G., Rahardjo, H., Gan, J. K.-M., 1–4 December 1987. Non-linearity of strength envelope for unsaturated soils. In: Proceedings of the 6th International Conference on Expansive Soils. New Delhi, India, pp. 49–54.

Fredlund, D. G., Xing, A., 1994. Equations for the soil-water characteristic curve. Canadian Geotechnical Journal 31 (4), 521–532.

Fredlund, D. G., Xing, A., Fredlund, M. D., Barbour, S. L., 1996. The relationship of the unsaturated soil shear strength functions to the soil-water characteristic curve. Canadian Geotechnical Journal 32, 440–448.

Frydman, S., 1964. The applicability of the Brazilian (indirect tension) test to soils. Australian Journal of Applied Science 15 (4), 335–343.

Gan, J. K. M., Fredlund, D. G., Rahardjo, H., 1988. Determination of the shear strength parameters of an unsaturated soil using the direct shear test. Can. Geotech. J. 25 (3), 500–510.

Gerard, P., Mahdad, M., McCormack, A. R., François, B., 2015. A unified failure criterion for unstabilized rammed earth materials upon varying relative humidity conditions. Construction and Building Materials 95, 437–447.

Hall, M., Allinson, D., 2009. Analysis of the hygrothermal functional properties of stabilised rammed earth materials. Building and Environment 44 (9), 1935–1942.

Hall, M., Djerbib, Y., 2004. Moisture ingress in rammed earth: Part 1 - the effect of soil particle-size distribution on the rate of capillary suction. Construction and Building Materials 18 (4), 269–280.

Hamblin, A. P., 1981. Filter paper method for routine measurement of field water potential. Journal of Hydrology 53 (3/4), 355–360.

Houben, H., Guillaud, H., 1996. Earth construction - a comprehensive guide., Second Edition. Intermediate Technology Publications, London (UK).

Jaquin, P. A., Augarde, C. E., Gallipoli, D., Toll, D. G., 2009. The strength of unstabilised rammed earth materials. Géotechnique 59 (5), 487–490.

Khalili, N., Khabbaz, M. H., 1998. A unique relationship for χ for the determination of the shear strength of unsaturated soils. Géotechnique 48 (6), 681–687.

Li, D., Wong, L. N. Y., 2013. The Brazilian disc test for rock mechanics applications: Review and new insights. Rock Mechanics and Rock Engineering 46 (2), 269–287.

McGregor, F., Heath, A., Maskell, D., Fabbri, A., Morel, J.-C., 2015. A review on the buffering capacity of earth building materials. Construction Materials.

NZS, 1998. NZS 4297:1998. Engineering design of earth buildings.

Panayiotopoulos, K. P., 1996. The effect of matric suction on stress-strain relation and strength of three alfisols. Soil and Tillage Research 39 (1-2), 45–59.

Powrie, W., 2008. Soil Mechanics: Concepts and Applications, 2nd Edition. Spon Press.

Standards Australia, 2003. AS1289.5.2.1.-2003. Methods of testing soils for engineering purposes. Method 5.2.1: Soil compaction and density testsDetermination of the dry density/moisture content relation of a soil using modified compactive effort.

Vanapalli, S. K., Fredlund, D. G., Pufahl, D. E., Clifton, A. W., 1996. Model for the prediction of shear strength with respect to soil suction. Can. Geotech. J. 33 (3), 379–392.

Walker, P., Standards Australia, 2002. Hb 195: The Australian earth building handbook.

Appendix

Full EMC strength prediction

Derivation of Eqn 10 using Figure 15 for the full EMC method:

$$\begin{aligned} \tau_{f,pred} &= c' + \sigma_{f,pred} \tan\phi' + \psi \tan\phi^b = \frac{\sigma_{c,pred}}{2}\cos\phi' && (12) \\ \sigma_{f,pred} &= \frac{\sigma_{c,pred}}{2}\left(1 - \sin\phi'\right) && (13) \end{aligned}$$

Substitute Eqn 13 into 12 to find UCS, $\sigma_{c,pred}$:

$$\begin{aligned} \frac{\sigma_{c,pred}}{2}\cos\phi' &= c' + \left(\frac{\sigma_{c,pred}}{2}\left(1 - \sin\phi'\right)\right)\tan\phi' + \psi\tan\phi^b && (14) \\ \sigma_{c,pred} &= 2\left(\frac{c' + \psi\tan\phi^b}{\cos\phi' - (1 - \sin\phi')\tan\phi'}\right) && (15) \end{aligned}$$

(Insert Figure 15 somewhere near here)

EMC strength prediction using circle maxima

Derivation of Eqn 11 using Figure 10 for the EMC method using circle maxima:

$$\begin{aligned} \tau_{f,pred} &= c' + \sigma_{f,pred}\tan\phi^* + \psi\tan\phi^B = \frac{\sigma_{c,pred}}{2} && (16) \\ \sigma_{f,pred} &= \frac{\sigma_{c,pred}}{2} && (17) \end{aligned}$$

Substitute Eqn 17 into 16 to find UCS, $\sigma_{c,pred}$:

$$\begin{aligned} \frac{\sigma_{c,pred}}{2} &= c' + \left(\frac{\sigma_{c,pred}}{2}\right)\tan\phi^* + \psi\tan\phi^B && (18) \\ \sigma_{c,pred} &= 2\left(\frac{c' + \psi\tan\phi^B}{1 - \tan\phi^*}\right) && (19) \end{aligned}$$

(Insert Figure 16 somewhere near here)

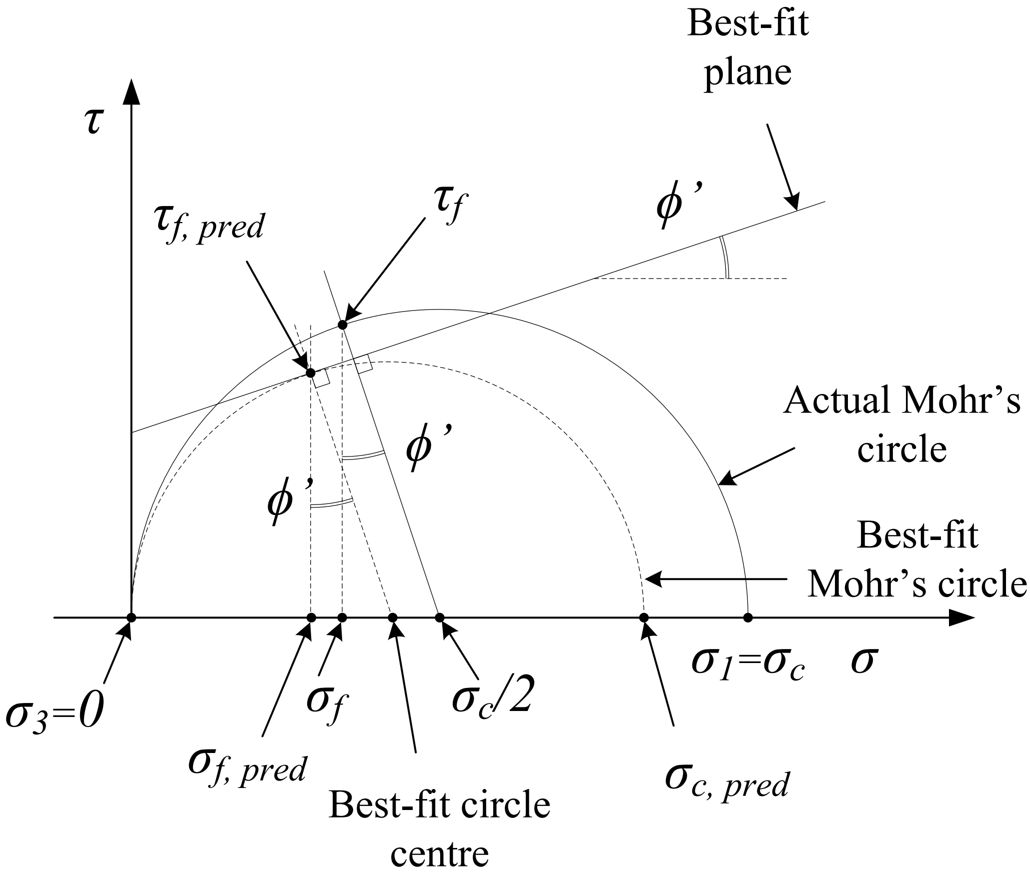

Figure 15: UCS calculation using full EMC method

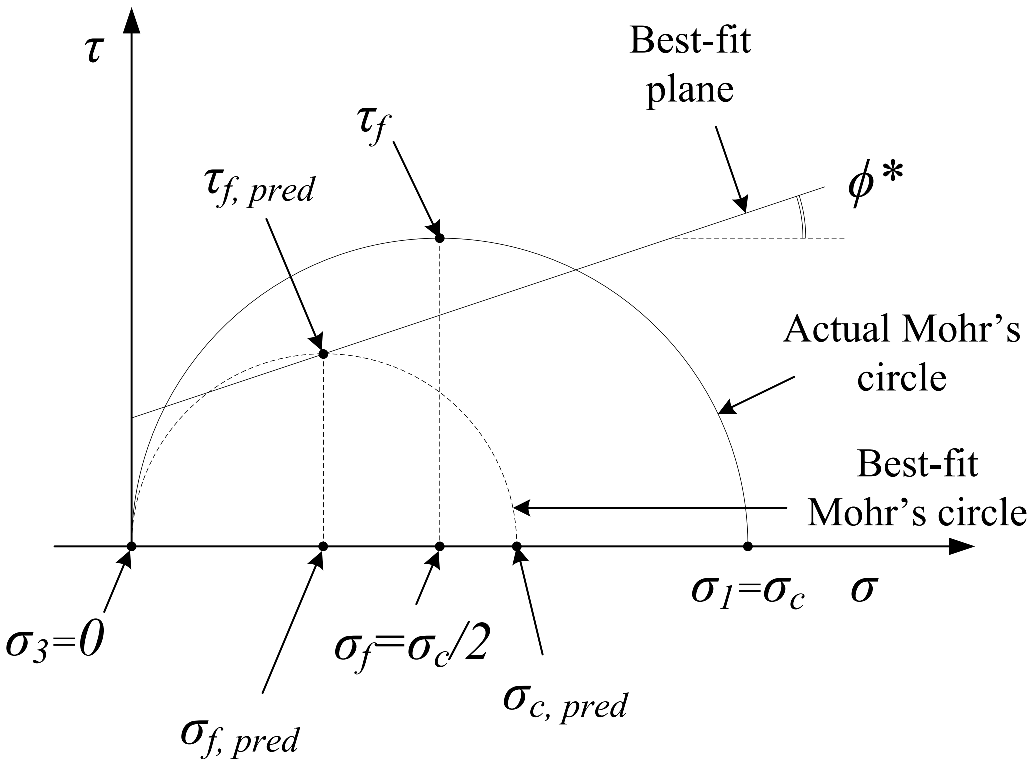

Figure 16: UCS calculation using full EMC method and circle maxima

Simplified EMC strength prediction

EMC parameter calculation using measured UCS and ITS values at plane corner points, using relationships shown in Figure 10:

$$\tan\phi_1^* = \frac{\sigma_{c1} + 4\sigma_{t1}}{\sigma_{c1} + 2\sigma_{t1}} \tag{20}$$

$$\tan\phi_2^* = \frac{\sigma_{c2} + 4\sigma_{t2}}{\sigma_{c2} + 2\sigma_{t2}} \tag{21}$$

$$\tan\phi^* = \frac{\tan\phi_1^* + \tan\phi_2^*}{2} \tag{22}$$

$$\tan\phi_c^b = \frac{\sigma_{c2} - \sigma_{c1}}{2\left(\psi_2 - \psi_1\right)} \tag{23}$$

$$\tan\phi_t^b = \frac{2\left(\sigma_{t1} - \sigma_{t2}\right)}{\psi_2 - \psi_1} \tag{24}$$

$$\tan\phi^b = \frac{\tan\phi_c^b + \tan\phi_t^b}{2} \tag{25}$$

where σ_c and σ_t are measured UCS and ITS values, subscripts t and c stand for tension and compression and subscripts 1 and 2 indicate the lower and upper suction values respectively. c' can be solved by rearranging Eqn 11:

$$c_1' = \frac{\sigma_c\left(1 - \tan\phi^*\right)}{2} - \psi\tan\phi^B \quad (\text{at } \psi_1) \tag{26}$$

$$c_2' = \frac{\sigma_c\left(1 - \tan\phi^*\right)}{2} - \psi\tan\phi^B \quad (\text{at } \psi_2) \tag{27}$$

$$c' = \frac{c_1' + c_2'}{2} \tag{28}$$

Note that σ_t is negative in Eqns 20 to 28.